Optimizing extraction methods by a comprehensive experimental approach and characterizing polyphenol compositions of *Ecklonia radiata*

Xinyu Duan [a], Vigasini Subbiah [b], Osman Tuncay Agar [a], Colin J. Barrow [b], Muthupandian Ashokkumar [c], Frank R. Dunshea [a,d], Hafiz A.R. Suleria [a,b,*]

[a] *School of Agriculture, Food and Ecosystem Sciences, Faculty of Science, The University of Melbourne, Parkville, VIC 3010, Australia*
[b] *Centre for Sustainable Bioproducts, School of Life and Environmental Sciences, Deakin University, Waurn Ponds, VIC 3217, Australia*
[c] *School of Chemistry, University of Melbourne, VIC 3010, Australia*
[d] *Faculty of Biological Sciences, The University of Leeds, Leeds, UK*

ARTICLE INFO

ABSTRACT

Brown seaweed *Ecklonia radiata* harbors valuable polyphenols, notably phlorotannins, prized for their health benefits. This study optimized phlorotannin extraction via conventional solvent extraction and ultrasound-assisted extraction methods, utilizing variable concentrations of ethanol. Employing fractional factorial designs, key variables were identified. Steepest ascent/descent method and central composite rotatable designs refined optimal conditions, enhancing phlorotannin and polyphenol yields, and antioxidant capacities. Under optimized conditions, phlorotannin contents reached 2.366 ± 0.01 and 2.596 ± 0.04 PGE mg/g, total polyphenol contents peaked at 10.223 ± 0.03 and 10.836 ± 0.02 GAE mg/g. Robust antioxidant activity was observed: DPPH and OH radical scavenging capacities measured 27.891 ± 0.06 and 17.441 ± 0.08 TE mg/g, and 37.498 ± 1.12 and 49.391 ± 0.82 TE mg/g, respectively. Reducing power capacities surged to 9.016 ± 0.02 and 28.110 ± 0.10 TE mg/g. Liquid chromatography-mass spectrometry (LC-MS) and high-performance liquid chromatography (HPLC) analyses revealed enriched antioxidant compounds. Variations in polyphenol profiles were noted, potentially influencing antioxidant capacity nuances. This study illuminated the potential of *E. radiata* potential as a polyphenol source and offers optimized extraction methods poised to benefit various industries.

1. Introduction

In various research endeavors aimed at isolating specific compounds from natural origins, traditional techniques remain prevalent, especially those utilizing liquid mediums such as organic solvents or combinations of water and organic solvents. Due to their operational simplicity, traditional extraction methods are commonly considered the most feasible choice for large-scale applications (Justino, Duarte, Freitas, Duarte, & Rocha-Santos, 2014). However, criticisms from researchers and industries persist regarding several drawbacks associated with these methods, including increased costs (e.g., time, energy, solvent usage), reduced selectivity and extraction efficiency, and the risk of environmental pollution stemming from the production of solvent residues (Garcia-Vaquero, Rajauria, & Tiwari, 2020). In addressing these challenges, various techniques have been developed to improve processing efficiency. These include the use of natural deep eutectic solvents

(NADES), as well as the application of microwave or ultrasonic fields (Cheng et al., 2023; Thakkar, Kachhwaha, & Kodgire, 2023; Xia et al., 2023).

Ultrasound-assisted extraction (UAE) relies heavily on the cavitation effect. As Lavilla and Bendicho (2017) have pointed out, ultrasonic waves induce pressure fluctuations in the extraction medium, leading to the formation and subsequent collapse of minuscule bubbles within plant matrices. This dynamic process generates localized hotspots and elevated pressure zones within the samples, effectively rupturing or deforming cell walls and facilitating the release of specific compounds into the solvent (Shen et al., 2023). Recent studies have highlighted the benefits of UAE over other advanced extraction technologies, including traditional solid-liquid extraction, microwave-assisted extraction, ultrasound–microwave-assisted extraction, hydrothermal-assisted extraction, and high-pressure-assisted extraction (Garcia-Vaquero et al., 2021). Of particular interest is the reduced extraction time

---

provided by UAE, which helps preserve compounds that are prone to degradation, hydrolysis, or oxidation (Shen et al., 2023). The extraction yield can vary depending on the extraction parameters and the biomass conditions such as species, season, and place of collection, whether using conventional solvent extraction (CSE) or UAE technology. While numerous studies have focused on optimizing extraction parameters, determining the most effective method remains elusive. No universal extraction method is considered ideal, as each extraction procedure is tailored to the specific characteristics of the plants. For example, a contrasting trend has been observed where traditional extraction methods yield higher extraction rates compared to UAE for two brown macroalgae, *Fucus vesiculosus* and *Pelvetia canaliculata* (Garcia-Vaquero et al., 2021).

Phlorotannins, a distinctive category of polyphenols, have been shown to possess intriguing antioxidant properties, which are primary mechanisms underlying various health-promoting benefits such as anti-inflammation and anti-diabetic effects (Duan, Agar, Barrow, Dunshea, & Suleria, 2023). Recently, studies have reported the extraction of phlorotannins from brown seaweed *F. vesiculosus* using NADES cooperated with UAE (Obluchinskaya et al., 2021). A total of 32 phlorotannins have been identified using high performance liquid chromatography-high resolution mass spectrometry (HPLC-HRMS) and tandem mass spectrometry (MS/MS) (Obluchinskaya et al., 2023), which represents a significant advancement in the characterization and understanding of the phlorotannin profile of this seaweed species. *Ecklonia*, a genus of kelp within the Lessoniaceae family, is also renowned for its rich concentration of eckol-type phlorotannins, which has attracted significant research attention in recent decades (Koirala, Jung, & Choi, 2017). Among its notable species is *Ecklonia radiata*, which thrives along the southern coastline of Australia, fostering biodiverse and productive ecosystems and providing essential support for a range of valuable ecosystem services (Bennett et al., 2015). In this case, a specific understanding of the phenolic profiles and their concentrations in *E. radiata* can offer advanced insights for its commercial development and further applications. However, there is a lack of detailed comparison on *E. radiata* among different extraction methods, regarding the selection of factors or the establishment of thresholds. Current research has mostly focused on obtaining phlorotannin-enriched fractions or individual isolated phlorotannins (Charoensiddhi, Conlon, Vuaran, Franco, & Zhang, 2017; Shrestha, Johnston, Zhang, & Smid, 2021). Therefore, the primary objective of this research was threefold: (i) to conduct a comparative analysis and enhancement of both methodologies using a systematic experimental approach that integrates fractional factorial design (FFD), steepest ascent/descent method, and central composite rotatable design (CCRD); (ii) to determine the levels of phlorotannin content and their associated antioxidant properties by employing spectrophotometric assays, with data obtained from 2,4-dimethoxybenzaldehyde (DMBA) assay, Folin-Ciocalteu's (FC) assay, 2,2-diphenyl-1-picrylhydrazyl (DPPH) assay, ferric ion reducing antioxidant power (FRAP) assay, and hydroxyl (•OH-) radical scavenging activity assay as response variables; and (iii) to quantify and characterize the polyphenolic compositions in the fractions using HPLC and liquid chromatography-mass spectrometry (LC/MS).

2. Materials and methods

2.1. Seaweed collection and extraction

Raw samples of *E. radiata*, a predominant brown seaweed species, were obtained in November (Summer) 2023 from Queenscliff Harbor (38°15′49.755″ S 144°40′4.471″ E) in Victoria, Australia. This species was selected due to its rich polyphenolic content and its ecological significance in the Great Southern Reef. The collection and pre-freezing procedure adhered to the methodology outlined in our prior research (Subbiah, Duan et al., 2023). The Deakin Marine Institute in Queenscliff, Victoria, Australia, successfully identified samples down to the species

level.

The extraction process utilized an ethanol-water mixtures with 0.1% formic acid, chosen for its effectiveness and lower environmental impact. Ethanol, in particular, is preferred for its efficiency in extracting a broad range of polyphenolic compounds and for its safety in both food and pharmaceutical applications, compared to other solvents like acetone and methanol (Li et al., 2017). These characteristics make ethanol particularly suitable for extracting natural antioxidants from seaweeds, where it maximizes the yield and quality of bioactive compounds. The extraction procedures of both methods were conducted as follows:

1) Conventional Solvent Extraction (CSE): 1 g of the powders was mixed with the solvent and placed in an incubator (OM11, Ratek Orbital Shaking Incubator, VIC, Australia).
2) Ultrasound-Assisted Extraction (UAE): 1 g of the powders was mixed with the solvent, followed by ultrasonication in an ice water bath using a cell disruptor (Branson, model Digital Sonifier 450 model).

All parameters were set up following the specifications detailed in section 2.3. Subsequently, the solid-liquid mixtures were subjected to centrifugation using a Hettich ROTINA380R centrifuge (Tuttlingen, Baden-Württemberg, Germany) at 7000 $\times g$ for 15 min at 4 °C. The supernatants were collected after centrifugation and stored at −20 °C.

2.2. Spectrophotometric assays

2.2.1. 2,4-Dimethoxybenzaldehyde (DMBA) assay

The quantification of phlorotannins content was conducted using the DMBA assay, following a methodology outlined in a prior study by Subbiah, Duan et al. (2023). The DMBA dye solution was prepared by mixing equal volumes of a DMBA solution in acetic acid (2%, *w/v*) and a hydrochloric acid (HCl) solution in acetic acid (6%, *v/v*). Phloroglucinol standard was dissolved in methanol (0–50 μg/mL) and employed for the measurements of total phlorotannin contents. The outcomes were reported as milligrams of phloroglucinol equivalents per gram of dry weight (PGE mg/g $_{d.w.}$). In brief, 25 μL of samples (or standards) were combined with 125 μL of DMBA dye solution in a 96-well microplate (Costar, Corning, NY). The mixture was then incubated for 60 min at 25 °C in the absence of light exposure. Subsequently, the absorbance was assessed at 510 nm employing a spectrophotometer (Thermo Fisher Scientific, Waltham, MA).

2.2.2. Folin-Ciocalteu's (FC) assay

The total polyphenol content (TPC) was roughly quantified through FC assays. The FC reagent was initially diluted with Milli-Q water at a ratio of 1:3 (*v/v*). Gallic acid standard was dissolved in methanol (0–200 μg/mL) and employed in constructing standard curve. The outcomes were quantified in milligrams of gallic acid equivalents per gram of dry weight (GAE mg/g $_{d.w.}$). Initially, 25 μL of samples (standards) were combined with 25 μL of FC reagent solution and 200 μL of Milli-Q water in a 96-well microplate. The mixture was subsequently incubated for 5 min at 25 °C in the absence of light exposure. Next, 25 μL of sodium carbonate (10%, *w/w*) was introduced into the reaction mixture, and the mixture was then subjected to a 60-min incubation period under identical conditions. Finally, the absorbance was assessed at a wavelength of 765 nm.

2.2.3. 2,2′-Diphenyl-1-picrylhydrazyl (DPPH) assay

The DPPH assay was employed to assess the antioxidant properties of the samples, specifically targeting their ability to scavenge radicals. The DPPH solution was prepared by dissolving 4 mg of DPPH powder in 100 mL of methanol of analytical grade. Trolox (6-hydroxy-2,5,7,8-tetramethylchroman-2-carboxylic acid) standard was dissolved in methanol to prepare gradient concentrations ranging from 0 to 200 μg/mL. The outcomes were expressed as milligrams of Trolox equivalents per gram

of dry weight (TE mg/g $_{d.w.}$). Initially, 25 μL of samples (or standards) were mixed with 275 μL of DPPH dye solution in a 96-well microplate, followed by a 30-min incubation at 25 °C in the absence of light exposure. Subsequently, the absorbance was measured at 517 nm.

2.2.4. Ferric ion reducing antioxidant power (FRAP) assay

Another essential mechanism exhibited by antioxidants is their capacity of reduction, as determined by the FRAP assay in the present investigation. The FRAP dye was prepared by mixing a 20 mM Fe [III] solution, a 10 mM 2,4,6-tri(2-pyridyl)-*s*-triazine (TPTZ) solution, and a 300 mM sodium acetate solution in a ratio of 1:1:10 (*v/v/v*). Same standard and concentrations were used as DPPH assays (Trolox in methanol solution with concentration ranging from 0 to 200 μg/mL). In summary, 20 μL of samples (or standards) were mixed with 280 μL of FRAP dye in a 96-well microplate, followed by a 10-min incubation at 37 °C in the absence of light exposure. The absorbance was then measured at a wavelength of 593 nm.

2.2.5. Hydroxyl radical (•OH-) scavenging assay

Hydroxyl radicals are among the most reactive and damaging oxygen-derived free radicals; thus, the capacity to scavenge or neutralize highly reactive hydroxyl radicals is of importance in evaluating antioxidants. Hydrogen peroxide was selected to simulate the presence of •OH-. Briefly, 50 μL of samples (or standards) were mixed with 50 μL hydrogen peroxide (6 mM) and 50 μL ferrous sulfate heptahydrate (6 mM) in a 96-well microplate, followed by 10-min incubation at 25 °C. Afterwards, 50 μL of 3-hydroxybenzoic acid (6 mM) was added as the trapping agent. The absorbance was then measured at a wavelength of 510 nm under 25 °C in the absence of light exposure. Trolox dissolved in methanol (0–1000 μg/mL) was used as standards.

2.3. Experimental procedure

2.3.1. Fractional factorial design

Fractional factorial designs (FFD) were devised to evaluate the influence of several independent variables on the total phlorotannin content, with DMBA serving as the response variable. Specifically, a 2^{5-1} and a 2^{4-1} design were applied, incorporating five and four independent variables, respectively, with low levels coded as −1 and high levels coded as +1. The selection of variables and their corresponding ranges was based on information provided in **Suppl 1** for both CSE and UAE extraction methods. These selections were guided by previous studies that identified these parameters as potentially significant factors influencing the extraction of phlorotannins and seaweed phenolic compounds (Lee, Xie, Duan, Ng, & Suleria, 2024; Vázquez-Rodríguez, Gutiérrez-Uribe, Antunes-Ricardo, Santos-Zea, & Cruz-Suárez, 2020).

2.3.2. Path of steepest ascent/descent

To expedite the process of narrowing down the optimal conditions' overall ranges through experimentation, the method of steepest ascent/descent was utilized. In the first-order model of FFD, the significant variables were systematically adjusted either downward or upward around the center points. The steepest ascent/descent direction is the one in which the response variable Y experiences the most rapid increase (decrease), and this direction is perpendicular to the contours of the fitted response surface (Liu et al., 2011). The parameters that were deemed insignificant or potentially significant were established at the central points of their corresponding variables. The detailed path of the steepest ascent/descent is presented in **Suppl 2**.

2.3.3. Central composite rotatable design

Central composite rotatable designs (CCRD) were implemented to assess the optimal extraction points. The selection of variables and parameter configurations were determined according to the outcomes derived from the FFD analysis and the steepest ascent/descent paths, as detailed in **Suppl 3**.

2.4. Characterization of polyphenol compositions by LC-ESI-QTOF-MS/MS

The instrumentation employed for the characterization of the polyphenol compositions in the optimized extracts consisted of the Agilent 1200 Infinity Series LC (Agilent Technologies, Santa Clara, CA) coupled with the Agilent 6520 Accurate-Mass Quadrupole Time-of-Flight MS QTOF (Agilent Technologies, Santa Clara, CA) and electrospray ionization (ESI) source. The total injection volume for each sample and mixed standard was 20 μL. The separation of polyphenols was performed using a Synergi Hydro-Reverse Phase 80°A, LC column (250 × 4.6 mm, 4 μm, Phenomenex, Torrance, CA) fitted with a C18 ODS guard column (Phenomenex, Torrance, CA) with an internal diameter of 4.0 × 2.0 mm. The gradient of 0.1% acetic acid in water (*v/v*, A) and 0.1% acetic acid in acetonitrile (*v/v*, B) at a constant flow rate of 0.3 mL/min was applied as follows: 0–4 min, 0–2% B; 4–10 min, 2–5% B; 10–50 min, 5–45% B; 50–52 min, 45–100% B; 52–58 min, 100% B; 58–60 min, 100–2% B; 60-70 min, 2% B. Both positive and negative modes were applied for peak identification. Nitrogen gas has been used as a nebulizer and drying gas at 45 psi, with a flow rate of 5 L/min at 300 °C. Capillary and nozzle voltage were placed at 3.5 kV and 500 V respectively and the mass spectra were obtained at the range of 50–1300 amu.

2.5. Determination of individual polyphenols by HPLC-DAD

2.5.1. Procedure of HPLC-DAD

Seven polyphenol standards were selected based on their potential presence in seaweed samples (Michalak et al., 2022). The compounds quantified in the study included phenolic acids such as gallic acid, sinapic acid, and syringic acid, flavonoids like (+)-catechin, (−)-epicatechin gallate, and (−)-epicatechin, as well as monomer phlorotannins, phloroglucinol. The HPLC system was an Agilent 1200 Series HPLC (Agilent Technologies, CA) featuring a diode-array detection (DAD) system. The column employed was identical to the one described in -QTOF-MS/MS section. The mobile phase consisted of (A) 0.1% acetic acid in water and (B) a mixture of acetonitrile/water (80:20, *v/v*) with 0.1% acetic acid, flowing at a rate of 1.0 mL/min. The injection volume of 20 μL remained consistent for both samples and standard compounds. The elution conditions applied were as follows: 0–20 min, 10% B; 20–30 min, 10–20% B; 30–35 min, 20–30% B, 35–45 min, 0% B (Rajauria, 2018). Absorbance readings were taken at wavelengths of 270 nm and 320 nm.

2.5.2. Method detection and quantification limits

The limit of detection (LOD) and limit of quantification (LOQ) were assessed through the measurement of the signal-to-noise ratio (S/N) of each standard compound individual peak. The LOD and LOQ were defined as the lowest concentration at which the signal-to-noise ratio reached or exceeded 3 and 10 (Rajauria, 2018).

$$LOD = 3.3R/S$$

$$LOQ = 10R/S$$

where R and S are the residual standard deviation of the regression line and slope of the calibration curve, respectively.

2.6. Statistical analysis

In all spectrophotometric assays, blank controls were subtracted (no samples but with the same volume of reagents and Milli-Q water). The absorbance of all samples was measured in triplicate to reduce potential bias and errors. ANOVA test of response values was carried out via XLSTAT (Addinsoft Inc. New York, NY, USA). Stat-Ease 360 software (version 22.0.3, Stat-Ease, Inc., MN) was used for the development of experimental designs (FFD and CCRD), regression analysis of

experimental data, conducting ANOVA tests of equations, and creating 3D response surface graphs. The statistical significance of the regression coefficient was assessed through an ANOVA test, which included performing an F-test at a confidence level of 95%. The 2D line figures were generated using Prism software (version 10.0.3, GraphPad Software,

MA). The adequacy of the fitted polynomial model was assessed by examining the coefficient of determination (R^2) and conducting a lack-of-fit test. The data acquisition and analysis for -MS/MS and HP were performed using Agilent Mass Hunter workstation software and the Waters Empower Window-based Software, respectively.
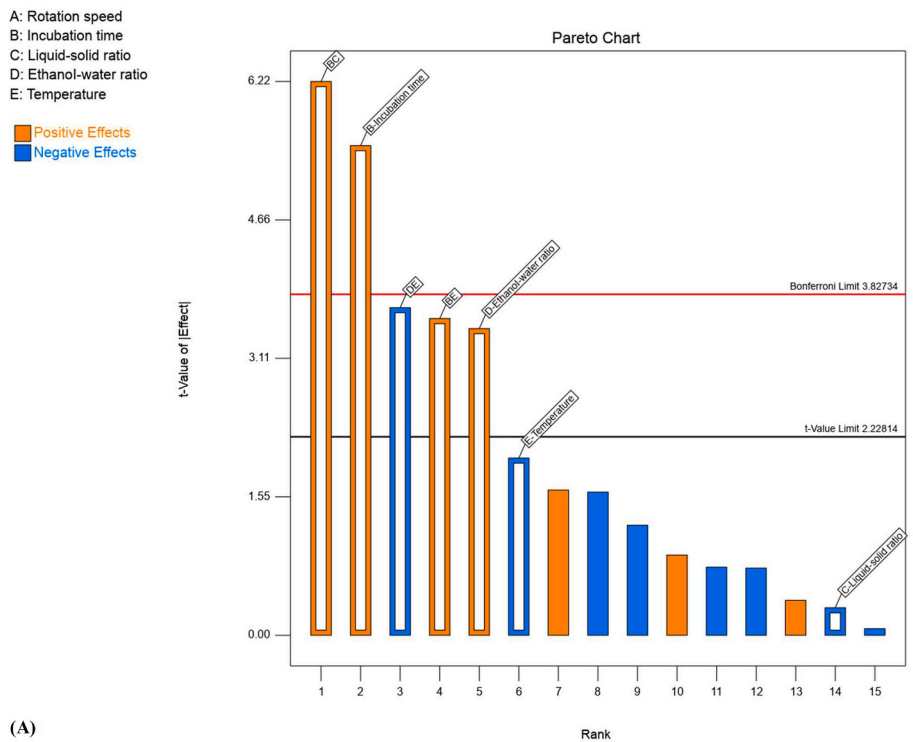
(A)
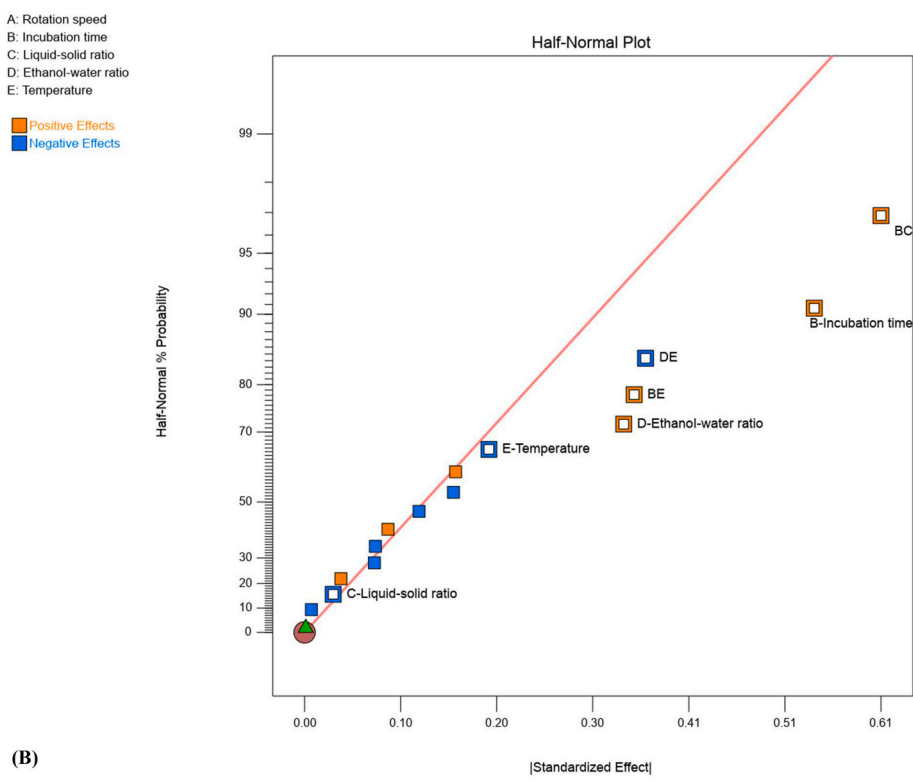
(B)

Fig. 1. (A) Pareto chart of conventional solvent extraction, (B) Half-normal plot of conventional solvent extraction, (C) Pareto chart of ultrasonic-assisted extraction, (D) half-normal plot of ultrasonic-assisted extraction.

A: Amplitude
B: Ultrasonic time
C: Liquid-solid ratio
D: Ethanol-water ratio

■ Positive Effects
■ Negative Effects

(C)

A: Amplitude
B: Ultrasonic time
C: Liquid-solid ratio
D: Ethanol-water ratio

■ Positive Effects
■ Negative Effects
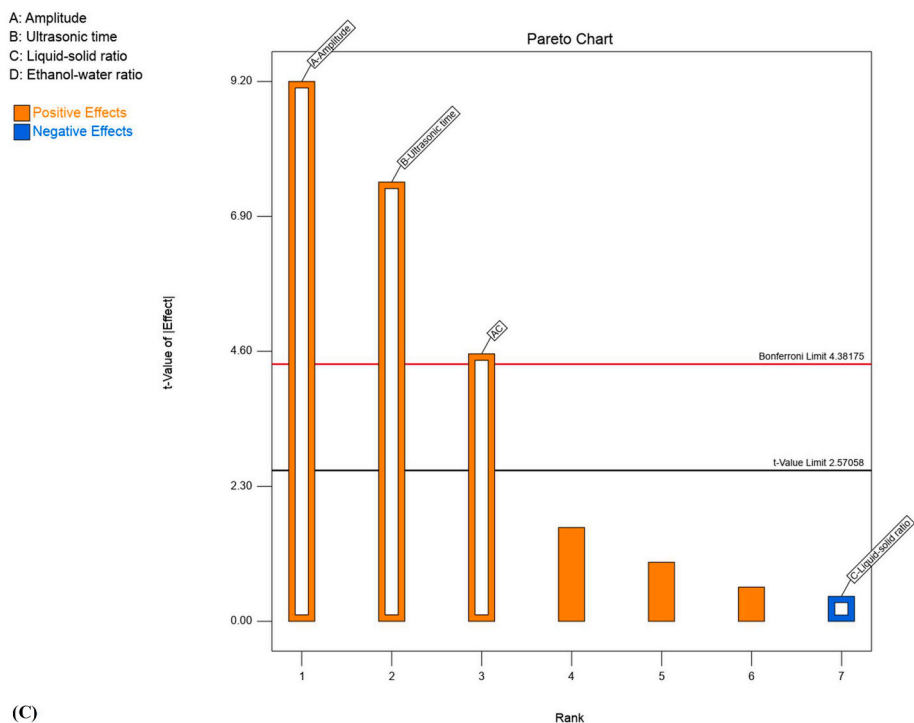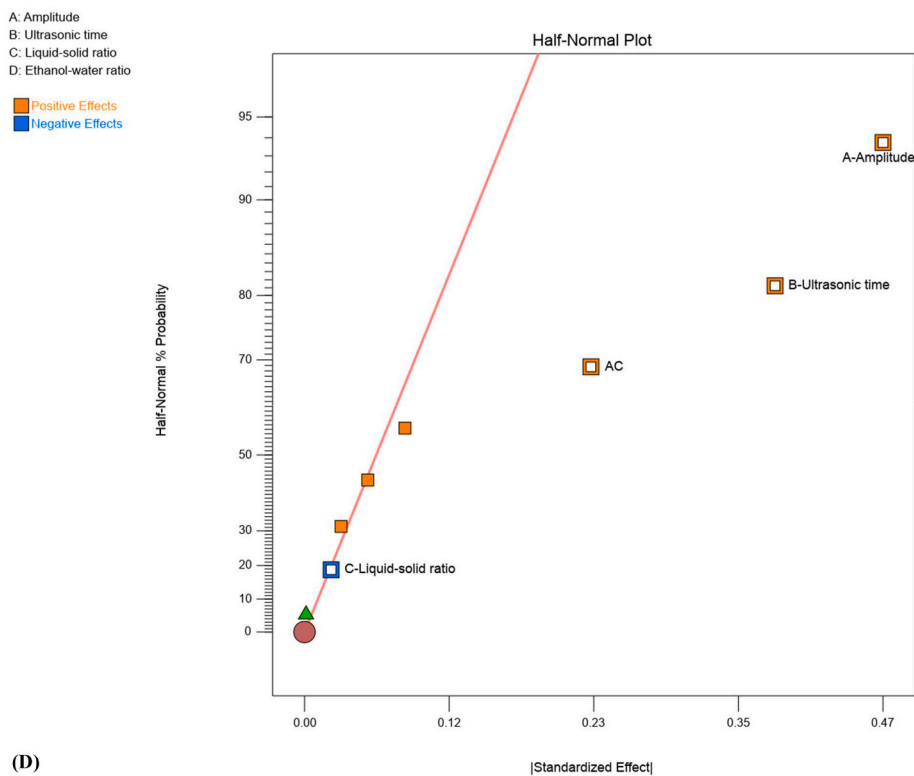
(D)

Fig. 1. (*continued*).

3. Results and discussion

3.1. Screening of significant variables using FFD

In this study, factorial mathematical models were performed using a 2^{5-1} design for CSE and a 2^{4-1} design for UAE, to systematically evaluate the relationship between the various extraction parameters and phlorotannin contents. Specifically, rotation speed, incubation time, incubation temperature, liquid-solid ratio, and ethanol-water ratio were selected for CSE analysis (Montesano & Gallo, 2023), while ultrasonic amplitude, ultrasonic time, liquid-solid ratio, and ethanol-water ratio were assessed for UAE (Altemimi, Watson, Choudhary, Dasari, & Lightfoot, 2016). The details of these designs and outcomes are documented in *Suppl 4* and *Suppl 5.* The impact of the variables on the responses (DMBA values for phlorotannin contents) was illustrated through Pareto charts and half-normal probability plots (*Fig. 1*).

Half-normal probability plots are pivotal for discerning significant from negligible effects in statistical analysis. The conspicuous red line, often referred to as the error line, delineates the lower 50% of effects, serving as a visual guide for effect selection. Factors that demonstrate more prominent and statistically significant influences on phlorotannin contents deviate noticeably from the trend line, whereas those with minor or insignificant effects typically closely follow the trend line (Javed & Asselin, 2020). *Fig.* 1 (B) demonstrates that both the duration of incubation and the ethanol-water ratio are significant factors in CSE in determining the phlorotannin levels in *E. radiata* extracts. Extended periods of incubation could potentially enhance the thorough extraction of the desired compounds from the plant. Conversely, extended periods of incubation may also lead to the oxidation and degradation of phenolics (Mokrani & Madani, 2016), which can be attributed to various factors such as exposure to light, the presence of oxygen, or enzymatic breakdown. The polarity of ethanol-water ratios varies, affecting their ability to solubilize phlorotannins. Compounds with an increased number of hydroxyl functional groups generally exhibit higher polarity, a characteristic that also applies to phlorotannins. Given the diverse linkages, polymerizations, and structural variations of phlorotannins, it is essential to carefully consider the choice of solvent polarity (Ford, Theodoridou, Sheldrake, & Walsh, 2019). Meanwhile, while two-factor interactions, such as time/liquid-solid ratio, ethanol-water ratio/temperature, and time/temperature, exerted a significant influence on the extraction efficiency, the individual factors of incubation temperature and liquid-solid ratio were determined to be statistically insignificant. Therefore, only single significant variables were considered in the following sections.

In the Pareto chart, the height of each bar reflects the standardized effects of the variables under investigation on the response values. The chart features two horizontal lines: the Bonferroni limit and the t-value limit, aiding in the evaluation of variable significance. A bar is deemed statistically significant ($p < 0.05$) if it surpasses both limits, while an effect falling below the t-value limit confirms insignificance ($p > 0.05$). The Pareto chart in *Fig.* 1 (A) provides a visual representation of the standardized effects of the variables on phlorotannin extraction, allowing for a clear differentiation of their significance. Variables that surpass the Bonferroni threshold (3.82734) are deemed to have a definitive impact on the response, as demonstrated by the time/liquid-solid ratio and incubation time, both exceeding this limit and thereby confirming their substantial role in the extraction efficiency of CSE. Interactions such as ethanol-water ratio/temperature and time/temperature, as well as the individual ethanol-water ratio factor, are observed between the Bonferroni and t-value limits (2.22814), suggesting potential significance that merits further consideration. This nuanced distinction between 'certain' and 'possible' significance can guide targeted adjustments in the extraction process to enhance yield and quality. The consistency between the Pareto chart and the half-normal probability plots reaffirms the robustness of the statistical model, evidenced by a satisfactory agreement between the adjusted R^2 (0.8666) and the predicted R^2 (0.6998), as detailed in **Suppl 6**. These findings underscore the importance of specific extraction parameters and their interactions in optimizing phlorotannin yield from *E. radiata*, facilitating a more focused approach in subsequent experimental designs.

In terms of UAE, results shown in. *Fig.* 1 (C) and (D) emphasized the significance of ultrasonic amplitude, treatment time, and the interaction between amplitude and liquid-solid ratio. Similar to CSE, only the two single factors mentioned were considered because of the minimal influence of the liquid-solid ratio. Undoubtedly, the amplitude of ultrasonic waves emerges as a critical determinant of cavitation intensity. Elevated amplitudes foster more vigorous cavitation phenomena, facilitating heightened disruption of cellular structures and potentially amplifying the extraction efficiency. However, it is imperative to note that excessively high amplitudes may induce elevated temperatures within the matrices, thereby diminishing the cavitation efficacy in the ultrasound-assisted extraction process (Kobus, Krzywicka, Starek-Wójcicka, & Sagan, 2022). An adjusted R^2 (0.9517) and the predicted R^2 (0.8300) met the reasonable agreement, with the difference <0.2 (**Suppl 6**).

3.2. Path of steepest ascent/descent

In the optimization process, multiple regression analysis was applied to the fractional factorial design (FFD) data, yielding first-order polynomial equations that describe the relationship between phlorotannin contents and extraction parameters for both conventional solvent extraction (CSE) and ultrasound-assisted extraction (UAE):

$$Y_{(CSE)} = 1.59 + 0.2691C2 + 0.1685C4 \tag{1}$$

$$Y_{(UAE)} = 1.46 + 0.2332U1 + 0.1897U2 \tag{2}$$

Here, Y represents the DMBA values indicating total phlorotannin contents, C2 is the incubation time, C4 is the ethanol-water ratio, U1 is the ultrasound amplitude, and U2 is the ultrasound time.

The trajectory of the steepest ascent/descent originated from the central point of the FFD design and followed a path where C2, C4, U1, and U2 varied in appropriate increments (as referred in **Suppl 2**). In both methods, the levels of phlorotannins initially increased, plateaued within the optimal range, and subsequently decreased as these variables were further elevated. It evidenced that the peak responses were observed at an incubation time of 870 min and an ethanol-water ratio of 80% in CSE, while an ultrasound time of 8.4 min and an amplitude of 140 W (35%) were confirmed in UAE, suggesting that these two points were near the region of maximum production responses.

3.3. Model fitting and response surface analysis by CCRD

The optimal levels of the key variables (C2, C4, U1 and U2) affecting phlorotannin contents, total polyphenol contents, and antioxidant activities were further explored using CCRD and Response Surface Methodology (RSM). The coded levels of selected variables are detailed in **Suppl 3**, with an extensive matrix and data available in **Suppl 7**.

In CSE trials, data were fitted to the mathematical model as per Eqs. (3–7), yielding high correlation coefficients (R^2) for all equations: 0.9452 in DMBA, 0.9641 for TPC, 0.9659 for DPPH, 0.9485 for FRAP, and 0.9393 for ●OH-, as shown in **Suppl 8**. The predicted R^2 values were in reasonable agreement with the adjusted values for all models. The fitness of predictive models was tested using the lack of fit test. The insignificant lack of fit values ($p > 0.05$) indicated the adequacy of the fitted models to predict the responses. The analysis of models highlighted that the incubation time (C2) had positive effects on all responses, while the ethanol-water ratio (C4) had no significant effect on DPPH radical scavenging activity. This was possibly because of the narrow range of water concentrations in the ethanol solvent, which aligns with the findings that between the ratios of 20% to 70%, there were no significant differences in IC_{50} values tested by the DPPH assay (Özbek, Halahlih, Göğüş, Koçak Yanık, & Azaizeh, 2020). However, single-factor self-interactions in the model equations suggested inconsistent impacts of ethanol-water ratios on DPPH values across different experimental conditions. Thus, these hierarchical terms were added to the regression equations after the backward elimination process because their influences were underestimated.

$$Y_{(CSE-DMBA)} = 2.35 + 0.0903C2 - 0.0761C4 + 0.0513C2 \times C4 - 0.1114C2^2 - 0.1182C4^2 \tag{3}$$

$$Y_{(CSE-TPC)} = 9.92 + 0.4169C2 - 0.7342C4 - 0.0272C2 \times C4 + 0.1964C2^2 - 0.6734C4^2 \tag{4}$$

$$Y_{(CSE-DPPH)} = 28.02 + 0.3304C2 - 0.0810C4 - 0.0710C2 \times C4 - 0.8593C2^2 - 1.02C4^2 \tag{5}$$

$$Y_{(CSE-FRAP)} = 8.74 + 0.3131C2 - 0.5769C4 - 0.1260C2 \times C4 - 0.2131C2^2 - 0.5808C4^2 \tag{6}$$

$$Y_{(CSE-OH)} = 37.34 - 0.2461C2 - 0.8081C4 + 0.7600C2 \times C4 - 1.47C2^2 + 0.4849C4^2 \tag{7}$$

$$Y_{(UAE-DMBA)} = 2.74 + 0.0215U1 + 0.0087U2 - 0.1422U1 \times U2 - 0.2184U1^2 - 0.1178U2^2 \tag{8}$$

$$Y_{(UAE-TPC)} = 10.51 + 0.1381U1 + 0.4734U2 - 0.1255U1 \times U2 - 0.5553U1^2 + 0.3192U2^2 \tag{9}$$

$$Y_{(UAE-DPPH)} = 17.45 + 1.12U1 - 0.0718U2 + 0.3340U1 \times U2 - 0.7710U1^2 - 0.3268U2^2 \tag{10}$$

$$Y_{(UAE-FRAP)} = 26.40 + 1.11U1 + 0.9973U2 - 0.1780U1 \times U2 - 0.5464U1^2 + 0.3846U2^2 \tag{11}$$

$$Y_{(UAE-OH)} = 46.42 + 1.50U1 + 1.94U2 + 2.64U1 \times U2 - 0.5198U1^2 - 0.2388U2^2 \tag{12}$$

In terms of UAE trials, similar high R^2 values were found in all equations (Eqs. 8–12), with 0.9579, 0.9442, 0.9438, 0.9495 and 0.9517 in four responses, respectively. Compared to CSE, more significant effects were triggered by two-factor interactions and single-factor self-interactions in UAE, which were also discovered in some other studies (Alasalvar & Yildirim, 2021; Oroian, Ursachi, & Dranca, 2020). It indicated that the combined effects of selected factors were not simply additive, as the impact of one factor depended on the level or presence of another factor. Ultrasound amplitude and time may exhibit synergistic effects and/or non-linear responses, meaning their combined influence on the outcome is greater or worse than the sum of their individual effects. Similar conclusions were drawn, as all individual and interacting parameters had a remarkable influence on the extraction process (Nath et al., 2022).

Three-dimensional (3D) plots depicting the predicted responses of the models were presented in Fig. 2 to more visual understand the non-linear interactions between parameters. In the analysis of the CSE figures, it was observed that the models displayed analogous trends with perfectly convex surfaces in both DMBA and DPPH responses. The optimal parameter configuration was situated at the midpoint of the two factors. It was anticipated that the DMBA and DPPH responses would achieve their maximum values when the incubation time ranged from 780 to 1050 min, and the ethanol-water ratio fell between 77 and 83%. It has been confirmed that a prolonged extraction time increases the extraction efficiency of bioactive compounds; however, there is a reduction over time when the threshold is reached (Brahmi et al., 2022). The decrease after the threshold time was also considered to be the result of decreased radical scavenging activities, as part of phlorotannins degraded. Interestingly, the figures of TPC, FRAP and ●OH- responses exhibited saddle and imperfect convex surfaces respectively, with the highest points at a low ethanol-water ratio and longer time setting. Moreover, when the incubation time was held constant, the impact of varying the ethanol-water ratio was readily apparent. This observation could be attributed to the increased water concentration's ability to enhance the extraction of specific polyphenols with higher solubility in water. Previous research has shown that using highly pure organic solvents can lead to cell dehydration and collapse, as well as the denaturation of cell wall proteins, which hinders the extraction of phenolic compounds (García, Rodríguez-Juan, Rodríguez-Gutiérrez, Rios, & Fernández-Bolaños, 2016). Nevertheless, when adjusting the ethanol-water ratio and modify the time, the impact may not be as pronounced. This is because a final equilibrium between the solute concentrations in the plant matrix and in the solvent might be reached after a certain time, leading to deceleration or stagnation in the extraction yield (Tan, Tan, & Ho, 2013).

The response of UAE-DMBA showed a similar central tendency trend as CSE, with the highest response value peaking at an amplitude of 120-160 W (30%–40%) and ultrasound time of 7.6–9.2 min. It was noticed that the intensity of ultrasound had a greater impact on the DPPH activity compared to the duration of treatment. This is because the main factor contributing to the improved extraction efficiency in UAE is the physical breakdown of cell structures, a process that is more directly affected by the intensity of ultrasound. Intriguingly, the surface was not consistent with TPC one, which decreased with increased amplitude. A feasible reason could be the structural changes of polyphenols under the treatment of ultrasound, as it has been demonstrated with proteins, pectin, and other polysaccharides (Huang, Ding, Li, & Ma, 2019; Qiu, Cai, Wang, & Yan, 2019). Likewise, elevated ultrasonic amplitudes have the potential to trigger the aggregation or polymerization of poly-phenols, culminating in the formation of larger molecular complexes and consequently reducing the apparent concentration of polyphenols. Studies have indicated that these intensified ultrasonic conditions can prompt conformational changes and aggregation phenomena, causing larger tannins to adopt more condensed or folded structures (e.g., tannin-protein affinity) as functional groups become obscured (McRae & Kennedy, 2011). Another possibility was considered due to the higher amplitude, which could result from the generation of free radicals within the cavitation bubbles. The formation of hydrogen peroxide may occur through the interaction of highly reactive hydroxyl radicals. These ultrasonic-assisted free radicals could potentially decrease the total phenols in the extract, rendering the phenolic compounds inaccessible for reaction with the FC reagent (Ho, Tan, Thoo, Abas, & Ho, 2014).

3.4. Verification of optimum conditions

Numerical optimization was performed with the aim of maximizing DMBA, TPC, DPPH, FRAP and ●OH- within the investigated range of extraction variables. Experiments were conducted to confirm the validity and adequacy of the predicted models with parameters adjusted according to equipment accuracy as follows: ethanol-water ratio at 77.9%, incubation time at 912 min, ultrasound amplitude at 39.142%
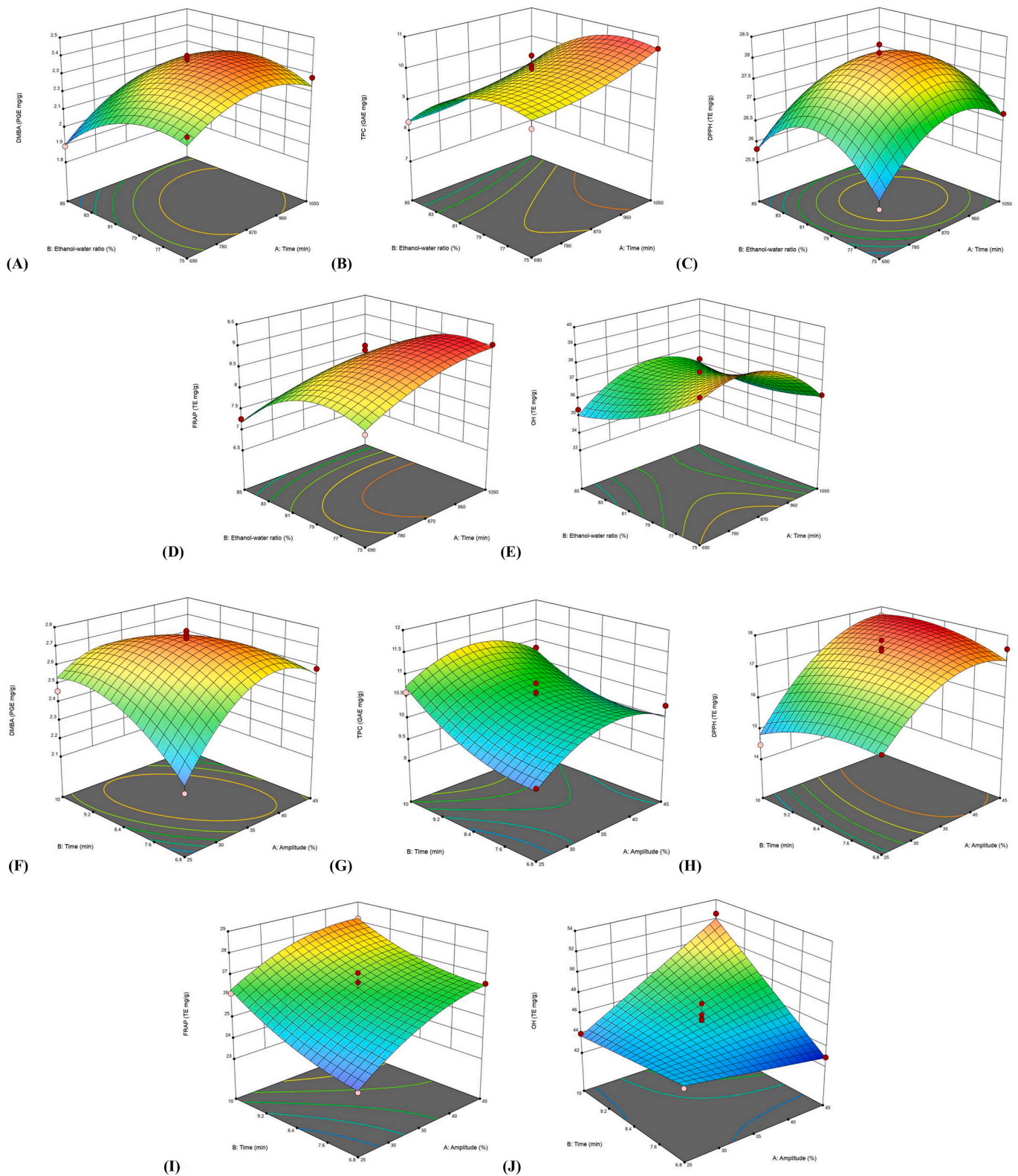
Fig. 2. 3D response surface plots demonstrate the significant interactive effects of independent variables for both conventional extraction (A-E) and ultrasonic-assisted extraction (F-J). The order of representation is estimated phlorotannin content (DMBA responses), total polyphenol content (TPC responses), radical scavenging activities (DPPH responses), and reducing power (FRAP responses), hydroxyl radical scavenging activities (OH responses).

(156.6 W), and ultrasound time at 9.8 min. Table 1 presented both the predicted and experimental values, all falling within the 95% confidence interval.

In our study, a lower amplitude was optimized compared to some

previous works, such as 400 W used on *Psidium cattleianum* levels (González-Silva et al., 2022), and 215 W/230 W applied to red/yellow tamarillo, respectively (Rohilla & Mahanta, 2021). Apart from inherent sample variations, temperature emerges as a crucial factor that can be

Table 1
Predicted and experimental values using optimized conditions.

	DMBA (PGE mg/g)		TPC (GAE mg/g)		DPPH (TE mg/g)		FRAP (TE mg/g)		•OH- (TE mg/g)		Desirability
	Pred.	Exp.	Pred.	Exp.	Pred.	Exp.	Pred.	Exp.	Pred.	Exp.	
CSE	2.369	2.366 ± 0.01	10.215	10.223 ± 0.03	27.922	27.891 ± 0.06	8.956	9.016 ± 0.01	37.537	37.498 ± 1.12	0.828
UAE	2.573	2.596 ± 0.04	11.100	10.836 ± 0.02	17.580	17.441 ± 0.08	27.896	27.710 ± 0.45	49.466	49.391 ± 0.82	0.732

readily modulated by adjusting the ultrasound amplitude. Free radical scavenging capacity increases steadily as ultrasonic temperature rises but likely decreases when it exceeds the threshold value (Vuong et al., 2014). It is evident that both the polyphenol contents and antioxidant capacity (except DPPH scavenging activity) in UAE were higher than CSE, consistent with previous research indicating that external ultrasonic waves enhanced the release of phenolic compounds from plant matrices, thereby relatively improved their antioxidant capacity (Ahmed et al., 2023). Paradoxically, lower DPPH values were observed in UAE, likely due to prolonged exposure to intense ultrasound waves, which can induce structural changes or degradation in certain antioxidants, especially those with higher degrees of polymerization or sensitivity to ultrasound treatment (Kumar, Srivastav, & Sharanagat, 2021). The generation of free radicals or disruption of conjugated double bonds has also been suggested (Foujdar, Bera, & Chopra, 2020). These alterations may result in fluctuations in radical scavenging, thereby explaining the results despite the higher overall phenolic content.

In comparison to our previous study, which reported a similar range of 10.16–12.87 GAE mg/g for the total polyphenol content of E. radiata

(Lee et al., 2024), our current study revealed a twofold increase in phlorotannin content. This notable difference could be attributed to variations in sample collection seasons. An illustration of this fact can be seen in the trade-off between resources allocation towards growth and reproduction, which may result in the reduced accumulation of bioactive compounds. For instance, previous research on E. radiata highlighted a significant inverse correlation between seaweed growth and changes in phlorotannin levels during spring, whereas no such relationship was observed during autumn (Steinberg, 1995), suggesting seasonal variations in the impact on bioactive compound synthesis. The concentration and composition of chemical compounds in seaweeds are greatly influenced by complex dynamic factors in their habitats, such as seasons, geolocation, ecological characterization, and biotic/abiotic changes (Lomartire et al., 2021). Study has shown higher crude and isolated phlorotannin contents during the summer-autumn period compared to the winter-spring period in Ecklonia cava subsp. stolonifera, with the lowest recorded at 2.9% of dry weight in March (Spring) and highest at 10.8% in August (Summer) (Sugiura et al., 2021). Additionally, remarkable differences have been found in the amount of

Table 2
Polyphenols tentatively identified in the extracts of Ecklonia radiata based on MS/MS fragmentation.

NO.	Observed (m/z)	Ionization (ESI$^+$/ ESI$^-$)	Product ion (m/z)	Molecular Formula	Proposed Compounds	Class	Samples
Phenolic acids							
1	387.1107	[M + H]$^+$	369, 195	$C_{20}H_{18}O_8$	5–5'-Dehydrodiferulic acid		UER
2	223.0871	** [M-H]$^-$	205, 163	$C_{11}H_{12}O_5$	Sinapic acid	*Hydroxycinnamic acids*	*CER, UER
3	355.1193	** [M-H]$^-$	193, 178, 149, 134	$C_{16}H_{20}O_9$	Ferulic acid 4-O-glucoside		*CER, UER
4	181.0492	[M-H]$^-$	166, 137, 135, 121	$C_9H_{10}O_4$	3-Hydroxy-3-(3-hydroxyphenyl) propionic acid	*Hydroxyphenylpropanoic acids*	UER
5	331.0891	**[M-H]$^-$	169, 125	$C_{13}H_{16}O_{10}$	Gallic acid 4-O-glucoside		UER
6	169.0166	[M-H]$^-$	125, 79	$C_7H_6O_5$	Gallic acid	*Hydroxybenzoic acids*	*CER, UER
7	197.0450	** [M-H]$^-$	182, 166, 138, 123	$C_9H_{10}O_5$	Syringic acid		CER
Flavonoids							
8	289.0722	[M-H]$^-$	245, 205, 179	$C_{15}H_{14}O_6$	(−)-Epicatechin		*UER, CER
9	865.1981	[M-H]$^-$	739, 713, 695	$C_{45}H_{38}O_{18}$	Procyanidin trimer C1	*Flavanols*	*UER, CER
10	441.0835	[M-H]$^-$	289, 169	$C_{22}H_{18}O_{10}$	(−)-Epicatechin gallate		UER
11	611.1386	**[M + H]$^+$	469, 311, 291	$C_{30}H_{26}O_{14}$	Prodelphinidin dimer B3		UER
12	596.1342	**[M + H]$^+$	287	$C_{30}H_{27}O_{13}$	Cyanidin 3-O-(6″-p-coumaroyl-glucoside)	*Anthocyanins*	UER
13	315.1022	**[M-H]$^-$	300, 285.135	$C_{17}H_{16}O_6$	Violanone	*Isoflavonoids*	UER
14	503.1217	[M + H]$^+$	255	$C_{24}H_{22}O_{12}$	6″-O-Malonyldaidzin		CER
15	431.1139	**[M-H]$^-$	413, 341, 311	$C_{21}H_{20}O_{10}$	Apigenin 6-C-glucoside	*Flavones*	UER
Other polyphenols							
16	261.0221	[M-H]$^-$	181, 97	$C_9H_{10}O_7S$	2-Hydroxy-4-methoxyacetophenone 5-sulfate	*Hydroxybenzoketones*	UER
17	211.0763	**[M-H]$^-$	167, 123, 105, 93	$C_{10}H_{12}O_5$	2,3-Dihydroxy-1-guaiacylpropanone		CER
18	331.2066	**[M-H]$^-$	287, 269	$C_{20}H_{28}O_4$	Carnosic acid	*Phenolic terpenes*	*CER, UER
19	165.0924	[M + H]$^+$	149, 137, 133, 124	$C_{10}H_{12}O_2$	2-Methoxy-5-prop-1-enylphenol	*Hydroxyphenylpropenes*	UER
Lignans							
20	417.1894	[M + H]$^+$	224, 193, 165	$C_{23}H_{28}O_7$	Schisandrol B	*Lignans*	CER
21	373.1429	**[M-H]$^-$	343, 313, 298, 285	$C_{20}H_{22}O_7$	7-Hydroxymatairesinol		*CER, UER
Phlorotannins							
22	495.0697	[M-H]$^-$	477, 371, 229	$C_{24}H_{15}O_{12}$	Tetramer	/	UER
23	747.0750	[M + H]$^+$	729, 711, 484, 571	$C_{36}H_{26}O_{18}$	Hexamer		*CER, UER

CER, conventional extracted *Ecklonia radiata*; UER, ultrasound-assisted extracted *Ecklonia radiata*; **, compounds detected in both negative and positive modes; *, compounds detected in more than one sample, while the data shown was from the sample marked with an asterisk.

phlorotannins among different individuals across broad latitudinal ranges, with seaweeds in higher latitudes capable of producing phlorotannins in a wider range of amounts, possibly as a response to environmental variables or stimuli, compared to algae in low latitude (Ank, Da Gama, & Pereira, 2019). This variability can also be explained by seaweed species and extraction procedure; for example, a wide range between 0.03 and 2.86 PGE mg/g was found within five brown seaweeds subjected to four pre-drying techniques, including *E. radiata* (Subbiah, Duan et al., 2023).

The antioxidant capacities of *E. radiata* exhibited a slight advantage compared to other brown seaweed species. Although significant differences were observed in the FRAP values between the two methods, both surpassed the values of the brown seaweed *Sargassum* sp. collected in Malaysia, which ranged from 7.81 ± 0.48 TE mg/g to 9.19 ± 0.43 TE mg/g (Norra, Aminah, Suri, & Zaidi, 2017). However, they also reported the effects of pre-boiling treatments, which notably increased the ferric reducing ability by approximately twofold. In another study, a remarkably low DPPH value of only 0.70 ± 0.12 TE mg/g was found using solid-liquid extraction, highlighting the limitations of conventional solvent extraction methods (Dinh, Saravana, Woo, & Chun, 2018). Consequently, ultrasound bath extraction was recommended, resulting in maximum DPPH values of 29.08 ± 0.80 TE mg/g across six different brown algae species (Dang, Bowyer, Van Altena, & Scarlett, 2018). Regarding the scavenging ability of •OH-, there is a lack of comparable data due to variations in protocols used. *E. radiata* demonstrated moderate performance, exhibiting a medium ability compared to other brown algae, with values ranging from 37.498 ± 1.12 TE mg/g to 49.391 ± 0.82 TE mg/g. Various extraction solvents yielded a range of values from 0.39 ± 0.35 TE mg/g to 134.49 ± 5.25 TE mg/g, with acetone showing superiority (Subbiah, Ebrahimi, et al., 2023). Though, ethanol is generally considered safer and more environmentally friendly than acetone, which can be toxic and requires proper handling and disposal.

3.5. Polyphenol composition analysis by LC-ESI-QTOF-MS/MS

3.5.1. Polyphenol composition

Polyphenols constitute a substantial group of secondary metabolites that confer antioxidant properties in plant sources. The increased focus on natural antioxidant is attributed to concerns regarding the potential adverse effects of synthetic antioxidants on the human enzyme system and DNA (Neha, Haider, Pathak, & Yar, 2019). Hence, LC-ESI-QTOF-MS/MS analysis was performed to assess and compare the polyphenol profiles of the two optimized extracts (***Suppl 9***). Table 2 presented a total of 23 polyphenols observed in this study, tentatively identified by considering their molecular weight, mass-to-charge ratio (m/z) of product ion, and by analyzing the mass information derived from their MS and MS/MS spectra in comparison with the MS spectral data and empirical formula generated by the Personal Compound Database and Library (PCDL), with a mass error of $\leq$10 ppm and a PCDL library score of $\geq$80.

In our study, two phenolic glycosides, including ferulic acid 4-*O*-glucoside (compound **3**) and gallic acid 4-*O*-glucoside (compound **5**), were discovered as phenolic acids. In the case of ferulic acid 4-*O*-glucoside, upon subjecting it to negative ESI mode (ESI⁻) in mass spectrometry, a deprotonated molecular ion was formed with a of m/z 355 (observed at m/z 355.1193). After the cleavage of the glycosidic bond linking the ferulic acid and glucose moieties, the deprotonated ferulic acid moiety was generated, exhibiting a characteristic m/z value of 193 (162 Da loss, indicative of a glucosyl residue). Afterwards, common fragmentation pathways observed for aromatic compounds involved a 15 Da loss ([M-H-•CH₃]⁻, m/z 178) and a 44 Da loss ([M-H-CO₂]⁻, m/z 149), corresponding to the removal of a methyl group and carbon dioxide, respectively. The last fragment detected at m/z 134 could potentially from the further loss of a methyl radical based on the fragment ion at m/z 149 (Liu et al., 2024). Similar ionization processes

were also observed in gallic acid 4-*O*-glucoside (deprotonated molecular ion [M-H]⁻ at m/z 331.0891), with deprotonated gallic acid moiety ([$C_7H_5O_5$]⁻, m/z 169) and further loss of carbon dioxide (CO_2, 44 Da). Other parent phenolic acids, such as sinapic acid (compound **2**, m/z 233.0871), gallic acid (compound **5**, m/z 169.0166), and syringic acid (compound **6**, m/z 197.0450), were also detected under ESI⁻ mode. According to the comprehensive summary (Cotas et al., 2020; Generalić Mekinić et al., 2019), all these phenolic acids were reported in previous studies of brown seaweeds (especially in the order Laminariales), either in their original forms, glucoside forms, or ester forms. They may also occur in more complex forms, such as the 5–5′-dehydrodiferulic acid (compound **1**, m/z 387.1107) identified in our study, which is formed by the oxidative coupling of two ferulic acid molecules. The product ion at m/z 369 corresponded to the loss of a water molecule ([M + H-H₂O]⁺, 18 Da), while the product ion at m/z 195 referred to the formation of a ferulic acid cation through the homolytic cleavage of the carbon-carbon bond between the two ferulic acid units. Moreover, 3-(3-hydroxyphenyl)-3-hydroxypropanoic acid (compound **4**, m/z 181.0492) is characterized as a dihydroxy monocarboxylic acid where 3-hydroxypropanoic acid is substituted by a 3-hydroxyphenyl group at position 3. Upon negative ionization, it lost a methyl radical ([M-H-•CH₃]⁻, leading to the generation of the product ion at m/z 166. Concurrently, the carboxyl group underwent decarboxylation ([M-H-CO₂]⁻), resulting in the formation of the product ion at m/z 137. The loss of formic acid (HCOOH) occurred due to a rearrangement followed by fragmentation, triggering the formation of product ion at m/z 135. Additionally, due to the simultaneous loss of a carbon dioxide (44 Da) and a hydroxyl radical (16 Da) from the deprotonated molecular ion, the product ion at m/z 121 was yielded. The data provided structural confirmation that aligned with the characteristics identified in a previous study of the analytes (Obrenovich et al., 2018).

In terms of flavonoids, a total of eight of them were detected in this study, including four subclasses as flavanols, anthocyanins, isoflavonoids, and flavones. In flavanols, both (−)-epicatechin (compound **8**, m/z 289.0722) and (−)-epicatechin gallate (compound **10**, m/z 441.0835) belong to polyphenolic compounds known as catechins. With well-known presence in green tea, they can also be found in various seaweed species, such as brown algae *Durvillaea antarctica* and *Macrocystis integrifolia* (Olate-Gallegos et al., 2019). Confirmed by the (−)-epicatechin MS/MS spectrum, the product ions were formed by the loss of carbon dioxide ([M-H-CO₂]⁻, m/z 245), flavonoid A ring ([M-H-C₄H₄O₂]⁻, m/z 205), and flavonoid B ring ([M-H-C₆H₅O₂]⁻, m/z 179) from the precursor ion at m/z 289. Likewise, the product ion at m/z 289 of (−)-epicatechin gallate was formed by the loss of a galloyl moiety ([M-H-C₇H₅O₅]⁻) from the deprotonated molecular ion [M-H]⁻, which was due to the cleavage of the ester bond between the galloyl group and the epicatechin core. Another fragment ion at m/z 169 corresponded to the deprotonated gallic acid [Gallic acid-H]⁻ (Escobar-Avello et al., 2019).

Aromatic sulfate esters are found as secondary metabolites in some plants that are formed through the sulfation of phenolic compounds, which involves adding a sulfate group to the hydroxyl group of the phenol. 2-Hydroxy-4-methoxyacetophenone 5-sulfate (compound **16**, m/z 261.0221) was tentatively identified in this study, with fragment ions at m/z 181 and 97. Based on the given information (Pan & Cheng, 2006), the product ion at m/z 181 is likely the result of the loss of the sulfate group ([M-H-OSO₃]⁻ from the parent compound. This is because the sulfate group is a good leaving group and can be easily cleaved from the parent compound during the fragmentation process. Meanwhile, due to the possibility of the cleavage of the oxygen-sulfur bond in the sulfate ester group, resulting the structure of hydrogen sulfate (HSO₄⁻, 97 Da).

Two phlorotannins were identified in the study: a tetramer phlorotannin (compound **22**, m/z 495.0697) and a hexamer (compound **23**, m/z 747.0750). Phlorotannins are primarily found in brown seaweed, with potentially minimal quantities in red algae (as no research article has been published on this topic yet) (Duan et al., 2023). The tetramer
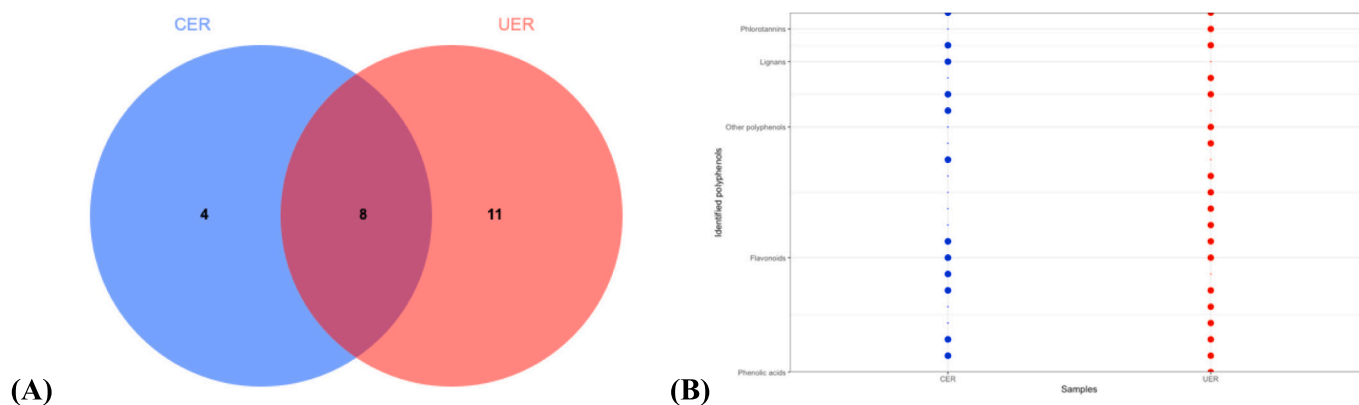
Fig. 3. (A) Venn diagram, (B) side-by-side dot plot diagram of the polyphenol compositions in two extracts.

comprised four units of phloroglucinols, yielding fragments at m/z 477, 371, and 229, respectively. Through a comparative analysis of prior experiments (Jacobsen, Sørensen, Holdt, Akoh, & Hermund, 2019), the phenomenon observed could potentially be attributed to the dissociation of a water molecule ($[M-H-H_2O]^-$, m/z 477), succeeded by fragmentation starting from the ether terminus ($[M-H-H_2O-C_6H_6O_3]^-$, m/z 371). Further loss of water molecules and phloroglucinol portions resulted in the formation of a product ion with an m/z of 229. The procedure was also contributed to a study on profiling phlorotannins (Lopes et al., 2018). As for the identified hexamer, it can be a phlorotannin compound composed of six units of phloroglucinol, with fragmentation patterns showing losses of one and two molecules of water ($[M-H-H_2O]^-$ of m/z at 729 and $[M-H-H_2O-H_2O]^-$ of m/z at 711), and further loss of phloroglucinol (126 Da, m/z 585) or simultaneous loss of phloroglucinol and methyl moieties (126 Da and 14 Da, m/z 571). This pattern was suggested to represent fucophlorethol with six (Ferreres et al., 2012); however, the entities demonstrate variances in size, degree of polymerization, and linkage diversity, thereby complicating their identification process.

3.5.2. Comparison of polyphenol composition

To delineate the polyphenol profiles of two extracts, comprehensive analyses were conducted utilizing a Venn diagram and a side-by-side dot plot (Fig. 3). The Venn diagram (Fig. 3A) highlights the distinct and common polyphenolic compounds identified in CER and UER, showcasing the specificity of each extraction technique. In CER, a total of 12 polyphenols were identified (4 unique and 8 shared), whereas UER revealed 19 polyphenols (11 unique and 8 shared). The chemical profiles of CER and UER display similarities, as the dot plot (Fig. 3B) indicates, mapping the occurrence of each polyphenol across the extracts.

Disparity in flavonoid content was the most pronounced, with CER exhibiting greater diversity compared to UER. This variation may be attributable to the differential effects of the extraction methods used, particularly the high-energy ultrasonic waves employed in UAE, which can affect the integrity of flavonoid structures. The intense energy and cavitation effects induced by ultrasound might contribute to the

degradation of flavonoids, resulting in diminished yields. The vigorous physical forces and localized elevated temperatures could potentially cause structural alterations or breakdown of these delicate compounds (Pingret, Fabiano-Tixier, & Chemat, 2013). Phenolic acids, in contrast, demonstrated a high degree of similarity between CER and UER, with a clustering of data points indicative of a consistent presence across both extraction types.

3.6. Quantification of selected polyphenols by HPLC-DAD

The HPLC-DAD analysis targeted seven polyphenols: phloroglucinol, (+)-catechin, (−)-epicatechin gallate, (−)-epicatechin, gallic acid, syringic acid and sinapic acid, quantified using authentic standards (as detailed in Table 3 and ***Suppl 10***). The proposed method was validated with respect to linearity, LOD and LOQ.

Linearity was assessed through linear regression analysis of the area against the concentration of five points (gradient concentrations) of each standard compound. The calibration curves exhibited strong linearity, as evidenced by correlation coefficients (r) ranging from 0.9920 to 0.9980, detailed in Table 3. The obtained HPLC data surpassed both LOD and LOQ thresholds, indicating detectable and quantifiable levels of the analytes.

Overall, UER exhibited higher concentrations of all detected polyphenols than CER, proving that ultrasonic assistance enhances the release of these compounds from the seaweed matrix. However, the effectiveness of ultrasound treatment can vary based on the specific characteristics of each polyphenol; some polyphenols are more amenable to UAE, which may account for the higher concentrations observed in UER. Interestingly, a reverse phenomenon was observed on seaweed *F. vesiculosus*, where higher concentrations were detected using conventional extraction with acetone. For instance, phloroglucinol (621.43 ± 7.29 μg/g > 494.32 ± 13.55 μg/g) and gallic acid (15.26 ± 0.95 μg/g > 6.87 ± 0.18 μg/g) exhibited this trend (Sánchez-Bonet et al., 2021). This could be attributed to the varying effects of different extraction solvents on interfering matrices, such as proteins and fibers, which may interact with polyphenolic compounds and ultimately affect

Table 3
Polyphenol quantification.

Peak No.	Compounds	Wavelength (nm)	Retention Time (min)	Standard Equation	R^2	Content (μg/g d.w.)		LOD (μg/mL)	LOQ (μg/mL)
						CER	UER		
1	Phloroglucinol	270	3.386	Y = 22,348× + 217.64	0.9943	135.6 ± 2.07	211.2 ± 1.06	0.27	0.83
2	Gallic acid	270	5.077	Y = 32,996×-155.78	0.9976	14.4 ± 0.51	15.7 ± 0.23	0.18	0.54
3	(+)-Catechin	270	16.560	Y = 3554.7×-50.43	0.9939	/	/	0.28	0.86
4	Syringic acid	270	27.013	Y = 47,986×-331.35	0.9978	16.9 ± 0.03	/	0.17	0.52
5	(−)-Epicatechin	270	30.384	Y = 18,288×-165.24	0.9920	29.3 ± 0.64	31.8 ± 0.42	0.33	0.99
6	(−)-Epicatechin gallate	270	35.159	Y = 12,574×-114.88	0.9980	34.0 ± 1.08	39.8 ± 0.51	0.16	0.50
7	Sinapic acid	320	38.792	Y = 51,402×-520.35	0.9967	24.3 ± 0.23	26.7 ± 0.17	0.21	0.63

their solubility and extraction efficiency.

Regarding the predominant polyphenol, phloroglucinol exhibited the highest concentrations in both extracts. Consistent with a study on brown seaweed *Himanthalia elongate*, although at a slightly higher concentration (394.1 ± 4.33 µg/g), phloroglucinol still represented the highest content among the quantified polyphenols (Rajauria, 2018). Phloroglucinol serves as a valuable standard for phlorotannin analysis due to its presence as a structural unit in many phlorotannin molecules. However, it is crucial to acknowledge that phlorotannins can manifest in various isomeric forms and polymerization degrees, potentially impacting their retention times and response factors.

Additionally, in our study, (+)-catechin was not detected, whereas (−)-epicatechin was found at 29.3 ± 0.64 µg/g and 31.8 ± 0.42 µg/g in both extracts, respectively. These concentrations align closely with a study on *F. vesiculosus*, which reported 31.01 ± 1.03 µg/g and 31.08 ± 1.47 µg/g in extracts using two methods (Sánchez-Bonet et al., 2021). However, they noted the presence of catechin, suggesting potential variations due to the differences in sample species.

4. Conclusion

In this study, we have meticulously developed a methodology for the efficient extraction of polyphenols, with a particular focus on phlorotannins sourced from the brown seaweed *E. radiata*. Our approach involved optimizing both conventional solvent extraction and ultrasound-assisted extraction techniques using step-by-step experimental designs such as fractional factorial design, the path of steepest ascent/descent, and central composite rotatable design. For convention extraction, the optimal condition was identified including a liquid-solid ratio of 20%, an incubation temperature of 25 °C, a rotation speed of 200 rpm, an ethanol-water ratio of 77.9%, and an incubation time of 912 min. Meanwhile, ultrasound-assisted extraction yielded best results with a liquid-solid ratio of 20%, an ethanol-water ratio of 70%, an ultrasound amplitude of 39.142% (equivalent to 156.6 W), and an ultrasound time of 9.8 min. Remarkably, the experimental values closely aligned with the predicted values under these optimized conditions. Subsequent LC-ESI-QTOF-MS/MS analysis unveiled the presence of 23 polyphenols in the optimized extracts, each showcasing distinct profiles between the two extraction methods. Complementary HPLC analysis further confirmed the prevalence of phloroglucinol alongside varying concentrations of other polyphenols like gallic acid, syringic acid, (−)-epicatechin, (−)-epicatechin gallate, and sinapic acid, with the notable absence of (+)-catechin. The findings strongly advocate for the superiority of ultrasonic-assisted extraction in terms of polyphenol yield. However, it is imperative to acknowledge the potential downside, as the elevated temperatures generated during ultrasound-assisted extraction may precipitate the degradation or alteration of certain phytochemicals. By adopting our optimized extraction protocols, industries can enhance their efficiency in obtaining valuable polyphenols from natural sources like brown seaweeds. Moreover, our findings underscore the importance of a balanced approach that prioritizes both yield enhancement and compound bioactivities, ensuring the quality of extracted polyphenols for diverse applications in pharmaceuticals, nutraceuticals, cosmetics, and food industries.

CRediT authorship contribution statement

Xinyu Duan: Writing – original draft, Software, Methodology, Formal analysis, Data curation, Conceptualization. **Vigasini Subbiah:** Formal analysis. **Osman Tuncay Agar:** Writing – review & editing, Supervision, Project administration. **Colin J. Barrow:** Supervision, Resources, Funding acquisition. **Muthupandian Ashokkumar:** Writing – review & editing, Supervision. **Frank R. Dunshea:** Supervision, Resources. **Hafiz A.R. Suleria:** Supervision, Resources, Project administration, Funding acquisition.

Declaration of competing interest

The authors declare that they have no known competing financial interests or personal relationships that could have appeared to influence the work reported in this paper.

Data availability

Data will be made available on request.

Appendix A. Supplementary data

Supplementary data to this article can be found online at https://doi.org/10.1016/j.foodchem.2024.139926.

References

Ahmed, H., Rashed, M. M., Almoiliqy, M., Abdalla, M., Bashari, M., Zaky, M. Y., … Wang, J. (2023). Antioxidant activity and total phenolic compounds of Commiphora gileadensis extracts obtained by ultrasonic-assisted extraction, with monitoring antiaging and cytotoxicity activities. *Food Science & Nutrition, 11*(6), 3506–3515.

Alasalvar, H., & Yildirim, Z. (2021). Ultrasound-assisted extraction of antioxidant phenolic compounds from Lavandula angustifolia flowers using natural deep eutectic solvents: An experimental design approach. *Sustainable Chemistry and Pharmacy, 22*, Article 100492.

Altemimi, A., Watson, D. G., Choudhary, R., Dasari, M. R., & Lightfoot, D. A. (2016). Ultrasound assisted extraction of phenolic compounds from peaches and pumpkins. *PLoS One, 11*(2), Article e0148758.

Ank, G., Da Gama, B. A. P., & Pereira, R. C. (2019). Latitudinal variation in phlorotannin contents from southwestern Atlantic brown seaweeds. *PeerJ, 7*, Article e7379.

Bennett, S., Wernberg, T., Connell, S. D., Hobday, A. J., Johnson, C. R., & Poloczanska, E. S. (2015). The 'great southern reef': Social, ecological and economic value of Australia's neglected kelp forests. *Marine and Freshwater Research, 67*(1), 47–56.

Brahmi, F., Mateos-Aparicio, I., Garcia-Alonso, A., Abaci, N., Saoudi, S., Smail-Benazzouz, L., Guemghar-Haddadi, H., Madani, K., & Boulekbache-Makhlouf, L. (2022). Optimization of conventional extraction parameters for recovering phenolic compounds from potato (Solanum tuberosum L.) peels and their application as an antioxidant in yogurt formulation. *Antioxidants, 11*(7), 1401.

Charoensiddhi, S., Conlon, M. A., Vuaran, M. S., Franco, C. M., & Zhang, W. (2017). Polysaccharide and phlorotannin-enriched extracts of the brown seaweed Ecklonia radiata influence human gut microbiota and fermentation in vitro. *Journal of Applied Phycology, 29*, 2407–2416.

Cheng, M., He, J., Li, C., Wu, G., Zhu, K., Chen, X., Zhang, Y., & Tan, L. (2023). Comparison of microwave, ultrasound and ultrasound-microwave assisted solvent extraction methods on phenolic profile and antioxidant activity of extracts from jackfruit (Artocarpus heterophyllus lam.) pulp. *LWT, 173*, Article 114395.

Cotas, J., Leandro, A., Monteiro, P., Pacheco, D., Figueirinha, A., Gonçalves, A. M., … Pereira, L. (2020). Seaweed phenolics: From extraction to applications. *Marine Drugs, 18*(8), 384.

Dang, T. T., Bowyer, M. C., Van Altena, I. A., & Scarlett, C. J. (2018). Comparison of chemical profile and antioxidant properties of the brown algae. *International Journal of Food Science & Technology, 53*(1), 174–181.

Dinh, T. V., Saravana, P. S., Woo, H. C., & Chun, B. S. (2018). Ionic liquid-assisted subcritical water enhances the extraction of phenolics from brown seaweed and its antioxidant activity. *Separation and Purification Technology, 196*, 287–299.

Duan, X., Agar, O. T., Barrow, C. J., Dunshea, F. R., & Suleria, H. A. (2023). Improving potential strategies for biological activities of phlorotannins derived from seaweeds. *Critical Reviews in Food Science and Nutrition,* 1–23.

Escobar-Avello, D., Lozano-Castellón, J., Mardones, C., Pérez, A. J., Saéz, V., Riquelme, S., … Vallverdú-Queralt, A. (2019). Phenolic profile of grape canes: Novel compounds identified by lc-esi-ltq-orbitrap-ms. *Molecules, 24*(20), 3763.

Ferreres, F., Lopes, G., Gil-Izquierdo, A., Andrade, P. B., Sousa, C., Mouga, T., & Valentão, P. (2012). Phlorotannin extracts from fucales characterized by HPLC-DAD-ESI-MS n: Approaches to hyaluronidase inhibitory capacity and antioxidant properties. *Marine Drugs, 10*(12), 2766–2781.

Ford, L., Theodoridou, K., Sheldrake, G. N., & Walsh, P. J. (2019). A critical review of analytical methods used for the chemical characterisation and quantification of phlorotannin compounds in brown seaweeds. *Phytochemical Analysis, 30*(6), 587–599.

Foujdar, R., Bera, M. B., & Chopra, H. K. (2020). Optimization of process variables of probe ultrasonic-assisted extraction of phenolic compounds from the peel of Punica granatum Var. Bhagwa and it's chemical and bioactivity characterization. *Journal of Food Processing and Preservation, 44*(1), Article e14317.

García, A., Rodríguez-Juan, E., Rodríguez-Gutiérrez, G., Rios, J. J., & Fernández-Bolaños, J. (2016). Extraction of phenolic compounds from virgin olive oil by deep eutectic solvents (DESs). *Food Chemistry, 197*, 554–561.

Garcia-Vaquero, M., Rajauria, G., & Tiwari, B. (2020). Conventional extraction techniques: Solvent extraction. In *Sustainable seaweed technologies* (pp. 171–189). Elsevier.

Garcia-Vaquero, M., Ravindran, R., Walsh, O., O'Doherty, J., Jaiswal, A. K., Tiwari, B. K., & Rajauria, G. (2021). Evaluation of ultrasound, microwave, ultrasound–microwave, hydrothermal and high pressure assisted extraction technologies for the recovery of phytochemicals and antioxidants from brown macroalgae. *Marine Drugs, 19*(6), 309.

Generalić Mekinić, I., Skroza, D., Šimat, V., Hamed, I., Čagalj, M., & Popović Perković, Z. (2019). Phenolic content of brown algae (Pheophyceae) species: Extraction, identification, and quantification. *Biomolecules, 9*(6), 244.

González-Silva, N., Nolasco-González, Y., Aguilar-Hernández, G., Sáyago-Ayerdi, S. G., Villagrán, Z., Acosta, J. L., … Anaya-Esparza, L. M. (2022). Ultrasound-assisted extraction of phenolic compounds from Psidium cattleianum leaves: Optimization using the response surface methodology. *Molecules, 27*(11), 3557.

Ho, S. K., Tan, C. P., Thoo, Y. Y., Abas, F., & Ho, C. W. (2014). Ultrasound-assisted extraction of antioxidants in Misai Kucing (Orthosiphon stamineus). *Molecules, 19*(8), 12640–12659.

Huang, L., Ding, X., Li, Y., & Ma, H. (2019). The aggregation, structures and emulsifying properties of soybean protein isolate induced by ultrasound and acid. *Food Chemistry, 279*, 114–119.

Jacobsen, C., Sørensen, A.-D-. M., Holdt, S. L., Akoh, C. C., & Hermund, D. B. (2019). Source, extraction, characterization, and applications of novel antioxidants from seaweed. *Annual Review of Food Science and Technology, 10*, 541–568.

Javed, T., & Asselin, E. (2020). Fe (III) precipitation and copper loss from Sulphate-chloride solutions at 150° C: A statistical approach. *Metals, 10*(5), 669.

Justino, C., Duarte, K., Freitas, A., Duarte, A., & Rocha-Santos, T. (2014). Classical methodologies for preparation of extracts and fractions. In *, Vol. 65. Comprehensive analytical chemistry* (pp. 35–57). Elsevier.

Kobus, Z., Krzywicka, M., Starek-Wójcicka, A., & Sagan, A. (2022). Effect of the duty cycle of the ultrasonic processor on the efficiency of extraction of phenolic compounds from Sorbus intermedia. *Scientific Reports, 12*(1), 8311.

Koirala, P., Jung, H. A., & Choi, J. S. (2017). Recent advances in pharmacological research on Ecklonia species: A review. *Archives of Pharmacal Research, 40*, 981–1005.

Kumar, K., Srivastav, S., & Sharanagat, V. S. (2021). Ultrasound assisted extraction (UAE) of bioactive compounds from fruit and vegetable processing by-products: A review. *Ultrasonics Sonochemistry, 70*, Article 105325.

Lavilla, I., & Bendicho, C. (2017). Fundamentals of ultrasound-assisted extraction. In *Water extraction of bioactive compounds* (pp. 291–316). Elsevier.

Lee, Z. J., Xie, C., Duan, X., Ng, K., & Suleria, H. A. (2024). Optimization of ultrasonic extraction parameters for the recovery of phenolic compounds in Brown seaweed: Comparison with conventional techniques. *Antioxidants, 13*(4), 409.

Li, Y., Fu, X., Duan, D., Liu, X., Xu, J., & Gao, X. (2017). Extraction and identification of phlorotannins from the brown alga, Sargassum fusiforme (Harvey) Setchell. *Marine Drugs, 15*(2), 49.

Liu, H., Agar, O. T., Imran, A., Barrow, C. J., Dunshea, F. R., & Suleria, H. A. (2024). LC-ESI-QTOF-MS/MS characterization of phenolic compounds in Australian native passion fruits and their potential antioxidant activities. *Food Science & Nutrition, 12*, 2455–2472.

Liu, S.-B., Qiao, L.-P., He, H.-L., Zhang, Q., Chen, X.-L., Zhou, W.-Z., Zhou, B.-C., & Zhang, Y.-Z. (2011). Optimization of fermentation conditions and rheological properties of exopolysaccharide produced by deep-sea bacterium Zunongwangia profunda SM-A87. *PLoS One, 6*(11), Article e26825.

Lomartire, S., Cotas, J., Pacheco, D., Marques, J. C., Pereira, L., & Gonçalves, A. M. (2021). Environmental impact on seaweed phenolic production and activity: An important step for compound exploitation. *Marine Drugs, 19*(5), 245.

Lopes, G., Barbosa, M., Vallejo, F., Gil-Izquierdo, Á., Andrade, P. B., Valentão, P., … Ferreres, F. (2018). Profiling phlorotannins from Fucus spp. of the northern Portuguese coastline: Chemical approach by HPLC-DAD-ESI/MSn and UPLC-ESI-QTOF/MS. *Algal Research, 29*, 113–120.

McRae, J. M., & Kennedy, J. A. (2011). Wine and grape tannin interactions with salivary proteins and their impact on astringency: A review of current research. *Molecules, 16*(3), 2348–2364.

Michalak, I., Tiwari, R., Dhawan, M., Alagawany, M., Farag, M. R., Sharun, K., … Dhama, K. (2022). Antioxidant effects of seaweeds and their active compounds on animal health and production–a review. *Veterinary Quarterly, 42*(1), 48–67.

Mokrani, A., & Madani, K. (2016). Effect of solvent, time and temperature on the extraction of phenolic compounds and antioxidant capacity of peach (Prunus persica L.) fruit. *Separation and Purification Technology, 162*, 68–76.

Montesano, D., & Gallo, M. (2023). 1.09 - sustainable approaches for the extraction and characterization of phytochemicals from food matrices. In P. Ferranti (Ed.), *Sustainable food science - a comprehensive approach* (pp. 103–118). Elsevier.

Nath, P. C., Bandyopadhyay, T. K., Mahata, N., Pabbi, S., Tiwari, O. N., Indira, M., & Bhunia, B. (2022). Optimization and kinetic study of ultrasonic-mediated phycoerythrin extraction from Anabaena sp. *Biomass Conversion and Biorefinery*, 1–12.

Neha, K., Haider, M. R., Pathak, A., & Yar, M. S. (2019). Medicinal prospects of antioxidants: A review. *European Journal of Medicinal Chemistry, 178*, 687–704.

Norra, I., Aminah, A., Suri, R., & Zaidi, J. A. (2017). *Effect of drying temperature on the content of fucoxanthin, phenolic and antioxidant activity of Malaysian brown seaweed* (Sargassum sp).

Obluchinskaya, E. D., Pozharitskaya, O. N., Shevyrin, V. A., Kovaleva, E. G., Flisyuk, E. V., & Shikov, A. N. (2023). Optimization of extraction of phlorotannins from the arctic fucus vesiculosus using natural deep eutectic solvents and their HPLC profiling with tandem high-resolution mass spectrometry. *Marine Drugs, 21*(5), 263.

Obluchinskaya, E. D., Pozharitskaya, O. N., Zakharova, L. V., Daurtseva, A. V., Flisyuk, E. V., & Shikov, A. N. (2021). Efficacy of natural deep eutectic solvents for extraction of hydrophilic and lipophilic compounds from Fucus vesiculosus. *Molecules, 26*(14), 4198.

Obrenovich, M. E., Donskey, C. J., Schiefer, I. T., Bongiovanni, R., Li, L., & Jaskiw, G. E. (2018). Quantification of phenolic acid metabolites in humans by LC–MS: A structural and targeted metabolomics approach. *Bioanalysis, 10*(19), 1591–1608.

Olate-Gallegos, C., Barriga, A., Vergara, C., Fredes, C., García, P., Giménez, B., & Robert, P. (2019). Identification of polyphenols from chilean brown seaweeds extracts by LC-DAD-ESI-MS/MS. *Journal of Aquatic Food Product Technology, 28*(4), 375–391.

Oroian, M., Ursachi, F., & Dranca, F. (2020). Influence of ultrasonic amplitude, temperature, time and solvent concentration on bioactive compounds extraction from propolis. *Ultrasonics Sonochemistry, 64*, Article 105021.

Özbek, H. N., Halahlih, F., Göğüş, F., Koçak Yanık, D., & Azaizeh, H. (2020). Pistachio (Pistacia vera L.) Hull as a potential source of phenolic compounds: Evaluation of ethanol–water binary solvent extraction on antioxidant activity and phenolic content of pistachio hull extracts. *Waste and Biomass Valorization, 11*, 2101–2110.

Pan, J.-Y., & Cheng, Y.-Y. (2006). Identification and analysis of absorbed and metabolic components in rat plasma after oral administration of 'Shuangdan'granule by HPLC–DAD–ESI-MS/MS. *Journal of Pharmaceutical and Biomedical Analysis, 42*(5), 565–572.

Pingret, D., Fabiano-Tixier, A.-S., & Chemat, F. (2013). Degradation during application of ultrasound in food processing: A review. *Food Control, 31*(2), 593–606.

Qiu, W.-Y., Cai, W.-D., Wang, M., & Yan, J.-K. (2019). Effect of ultrasonic intensity on the conformational changes in citrus pectin under ultrasonic processing. *Food Chemistry, 297*, Article 125021.

Rajauria, G. (2018). Optimization and validation of reverse phase HPLC method for qualitative and quantitative assessment of polyphenols in seaweed. *Journal of Pharmaceutical and Biomedical Analysis, 148*, 230–237.

Rohilla, S., & Mahanta, C. L. (2021). Optimization of extraction conditions for ultrasound-assisted extraction of phenolic compounds from tamarillo fruit (Solanum betaceum) using response surface methodology. *Journal of Food Measurement and Characterization, 15*, 1763–1773.

Sánchez-Bonet, D., García-Oms, S., Belda-Antolí, M., Padrón-Sanz, C., Lloris-Carsi, J. M., & Cejalvo-Lapeña, D. (2021). RP-HPLC-DAD determination of the differences in the polyphenol content of Fucus vesiculosus extracts with similar antioxidant activity. *Journal of Chromatography B, 1184*, Article 122978.

Shen, L., Pang, S., Zhong, M., Sun, Y., Qayum, A., Liu, Y., Rashid, A., Xu, B., Liang, Q., & Ma, H. (2023). A comprehensive review of ultrasonic assisted extraction (UAE) for bioactive components: Principles, advantages, equipment, and combined technologies. *Ultrasonics Sonochemistry, 106646*.

Shrestha, S., Johnston, M. R., Zhang, W., & Smid, S. D. (2021). A phlorotannin isolated from Ecklonia radiata, Dibenzodioxin-fucodiphloroethol, inhibits neurotoxicity and aggregation of β-amyloid. *Phytomedicine Plus, 1*(4), Article 100125.

Steinberg, P. D. (1995). Seasonal variation in the relationship between growth rate and phlorotannin production in the kelp Ecklonia radiata. *Oecologia, 102*, 169–173.

Subbiah, V., Duan, X., Agar, O. T., Dunshea, F. R., Barrow, C. J., & Suleria, H. A. (2023). Comparative study on the effect of different drying techniques on phenolic compounds in Australian beach-cast brown seaweeds. *Algal Research, 72*, Article 103140.

Subbiah, V., Ebrahimi, F., Agar, O. T., Dunshea, F. R., Barrow, C. J., & Suleria, H. A. (2023). Comparative study on the effect of phenolics and their antioxidant potential of freeze-dried Australian beach-cast seaweed species upon different extraction methodologies. *Pharmaceuticals, 16*(5), 773.

Sugiura, Y., Kinoshita, Y., Misumi, S., Yamatani, H., Katsuzaki, H., Hayashi, Y., & Murase, N. (2021). Correlation between the seasonal variations in phlorotannin content and the antiallergic effects of the brown alga Ecklonia cava subsp. stolonifera. *Algal Research, 58*, Article 102398.

Tan, M., Tan, C., & Ho, C. (2013). Effects of extraction solvent system, time and temperature on total phenolic content of henna (Lawsonia inermis) stems. *International Food Research Journal, 20*(5), 3117.

Thakkar, K., Kachhwaha, S. S., & Kodgire, P. (2023). Enhanced castor seed oil extraction assisted by the synergistic effect of ultrasound and microwave: Impact on extraction effectiveness and oil quality. *Chemical Engineering and Processing Process Intensification, 185*, Article 109307.

Vázquez-Rodríguez, B., Gutiérrez-Uribe, J. A., Antunes-Ricardo, M., Santos-Zea, L., & Cruz-Suárez, L. E. (2020). Ultrasound-assisted extraction of phlorotannins and polysaccharides from Silvetia compressa (Phaeophyceae). *Journal of Applied Phycology, 32*, 1441–1453.

Vuong, Q. V., Goldsmith, C. D., Dang, T. T., Nguyen, V. T., Bhuyan, D. J., Sadeqzadeh, E., … Bowyer, M. C. (2014). Optimisation of ultrasound-assisted extraction conditions for phenolic content and antioxidant capacity from Euphorbia tirucalli using response surface methodology. *Antioxidants, 3*(3), 604–617.

Xia, B., Liu, Q., Sun, D., Wang, Y., Wang, W., & Liu, D. (2023). Ultrasound-assisted deep eutectic solvent extraction of polysaccharides from Anji white tea: Characterization and comparison with the conventional method. *Foods, 12*(3), 588.